

DESY 16-121, DO-TH 16/25

## The new ABMP16 PDFs

---

### Sergey Alekhin<sup>\*†</sup>

*II. Institut für Theoretische Physik, Universität Hamburg, Luruper Chaussee 149, D-22761 Hamburg, Germany;*  
*Institute for High Energy Physics, 142281 Protvino, Russia*  
E-mail: [sergey.alekhin@desy.de](mailto:sergey.alekhin@desy.de)

### Johannes Blümlein

*Deutsches Elektronensynchrotron DESY, Platanenallee 6, D-15738 Zeuthen, Germany*  
E-mail: [Johannes.Bluemlein@desy.de](mailto:Johannes.Bluemlein@desy.de)

### Sven-Olaf Moch

*II. Institut für Theoretische Physik, Universität Hamburg, Luruper Chaussee 149, D-22761 Hamburg, Germany*  
E-mail: [sven-olaf.moch@desy.de](mailto:sven-olaf.moch@desy.de)

### Ringaile Plačakytė

*Deutsches Elektronensynchrotron DESY, Notkestraße 85, D-22607 Hamburg, Germany*  
E-mail: [ringaile.placakyte@desy.de](mailto:ringaile.placakyte@desy.de)

We present an update of the ABM12 PDF analysis including improved constraints due to the final version of the inclusive DIS HERA data, the Tevatron and LHC data on the  $W$ - and  $Z$ -production and those on heavy-quark production in the electron- and neutrino-induced DIS at HERA and the fixed-target experiments NOMAD and CHORUS. We also check the impact of the Tevatron and LHC top-quark production data on the PDFs and the strong coupling constant. We obtain  $\alpha_s(M_Z) = 0.1145(9)$  and  $0.1147(8)$  with and without the top-quark data included, respectively.

*XXIV International Workshop on Deep-Inelastic Scattering and Related Subjects*  
*11-15 April, 2016*  
*DESY Hamburg, Germany*

---

<sup>\*</sup>Speaker.

<sup>†</sup>This work was supported in part by the European Commission through contract PITN-GA-2012-316704 (HIGGS-TOOLS).

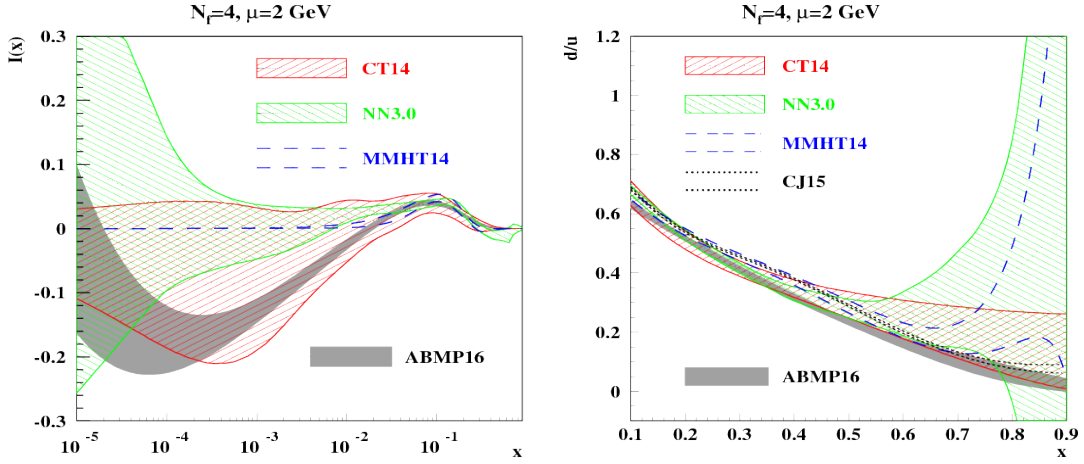


**Figure 1:** Left: The  $1\sigma$  error band for the NNLO iso-spin asymmetry of the sea  $I(x)$  for the 4-flavor scheme at the scale  $\mu = 2$  GeV as a function of the Bjorken  $x$  obtained in the present fit (gray shaded area) in comparison with the corresponding ones obtained in the CT14 [3] (red right-tilted hatch), MMHT14 [4] (blue dashed lines), and NNPDF3.0 [5] (green left-tilted hatch) analyses. Right: The same for the ratio  $d/u$  with the NLO CJ15 results [6] added.

A steady progress in accumulating and processing hard-scattering data from Tevatron, HERA, and the LHC stimulates an improvement in determining parton distribution functions (PDFs). In particular, a bulk of the data on  $W$ - and  $Z$ -boson production obtained recently at the Tevatron collider and the LHC opens a realistic perspective of using the Drell-Yan (DY) data as a powerful constraint to disentangle quark flavors. The overall DY statistics accumulated by the Tevatron and LHC experiments provides a typical uncertainty in the data of  $O(1\%)$  that is competitive to the most accurate deep-inelastic-scattering (DIS) data sets available. The DY data at large  $W$ - and  $Z$ -boson rapidity are particularly suitable to study the PDFs at small and large values of Bjorken variable  $x$  probed in case of asymmetric kinematics. These benefits are employed in the updated version of the ABM12 PDF analysis [1] including the most accurate DY data from Tevatron and the LHC. These data are reasonably well accommodated in the ABM12 fit, with a typical value of  $\chi^2 \lesssim 1.5$  per data point, cf. Table 1. In combination with the existing DIS data from HERA and the fixed-target experiments they allow to separate the contribution from  $u$ - and  $d$ -quarks in a wide range of  $x \simeq 10^{-4} \div 0.9$ . This input is particularly useful for the extraction of the  $d$ -quark distribution at large  $x$  since it allows to avoid uncertainties due to the modeling of nuclear effects, which appear in case of employing the DIS deuteron data for this purpose. The statistical accuracy of the  $d$ -quark distribution, which can be achieved using the DY data is comparable to the one for the existing DIS deuteron data sets used earlier in the ABM12 fit [2]. Therefore, in the present analysis we skip the latter in order to reduce theoretical uncertainties keeping the overall one on the same level, cf. Fig. 1. The forward DY data also help to disentangle the sea quark distributions at small  $x$ . In particular this concerns the shape of the isospin asymmetry  $I(x) = x[\bar{d}(x) - \bar{u}(x)]$  now parameterized in a model-independent way allowing to release a constraint  $I(x) \sim x^{0.7}$  imposed in the ABM12 fit. This constraint has been motivated by Regge-phenomenology arguments valid asymptotically for  $x \rightarrow 0$ . However, an explicit onset of this asymptotic is not easily specified and has to be extracted

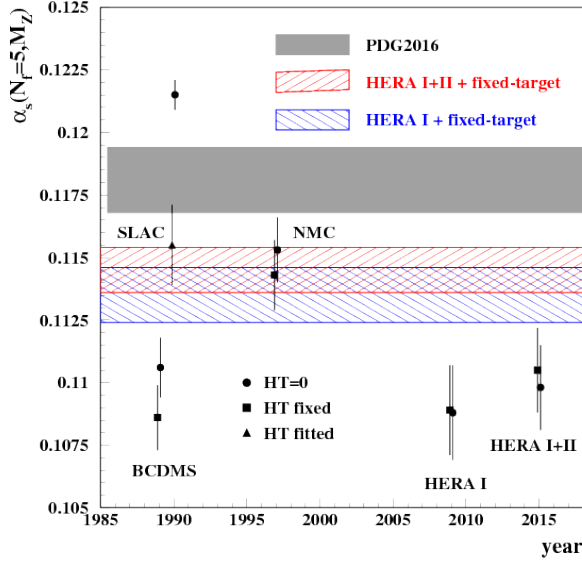


**Figure 2:** The value of  $\alpha_s$  preferred by various DIS data samples employed in present analysis w.r.t. the year of data publication. Three variants of the fit with different treatment of the HT terms are presented: HT set to 0 or to the ones obtained in the combined fit (circles and squares, respectively) and fitted to the one particular data set (triangles). The  $\alpha_s$  bands obtained by using the combination of the fixed-target SLAC, BCDMS, and NMC samples with the ones from the HERA Run-I (left-tilted hatches) and the Run-I+II (right-tilted hatches) as well as the PDG average [10] are given for comparison.

from the experimental data. Releasing the Regge-like constraint on  $I(x)$ , we observe a substantial deviation from 0 at  $x \sim 10^{-4}$  and a turnover of this trend at smaller  $x$  that still allows for a Regge-like shape at  $x \sim 10^{-6}$ . Determinations of the sea iso-spin asymmetry obtained in the CT14 [3], MMHT14 [4], and NNPDF3.0 [5] PDF fits are in a broad agreement with our results although the uncertainties obtained by other groups are much bigger than ours because of fewer data used, cf. Fig. 1 and Table 1. The strange quark distribution determined from a global PDF fit is commonly separated from the non-strange ones using the data on charm production in neutrino-induced DIS. In the present analysis the strange sea is refined as compared to ABM12 due to the addition of the recent NOMAD and CHORUS data. The former allows to pin down the strange sea at large  $x$ , where other experiments are not conclusive and the latter provides a unique information about the charm-production dynamics, being not sensitive to details of modeling its fragmentation [9]. The resulting strange sea suppression factor updated is  $\kappa(20 \text{ GeV}^2) = 0.658 \pm 0.026$  for the 3-flavor PDFs. Furthermore the updated PDF predictions were compared to the ATLAS and CMS data on associated 'W+charm' production and good agreement was found at NLO in QCD.

The value of the strong coupling constant  $\alpha_s(M_Z)$  is extracted in the present analysis simultaneously with the PDFs and the heavy-quark masses, similarly to the ABM12 case. Basically, it is controlled by the inclusive DIS data from the fixed-target experiments and the HERA collider. The values preferred by each particular data set are displayed in Fig. 2 in a chronological order. The most recent data set in this row stems from a combination of the H1 and ZEUS measurements performed during Run I and Run II of the HERA collider operation. The value of  $\alpha_s$  preferred by these data is relatively small as compared to the PDF world average [10], however it is somewhat larger than the one obtained from the Run I HERA combination. As a result the NNLO value of  $\alpha_s(M_Z) = 0.1145 \pm 0.0009$  obtained in the present analysis is by  $1\sigma$  bigger than the earlier ABM12 result based on the Run I HERA data. Earlier DIS data prefer bigger values of  $\alpha_s$ , cf. Fig. 2 and they are also more sensitive to the impact of higher-twist (HT) contribution to the DIS structure functions. The HT terms were studied in detail earlier [11] and were found to be non-negligible for

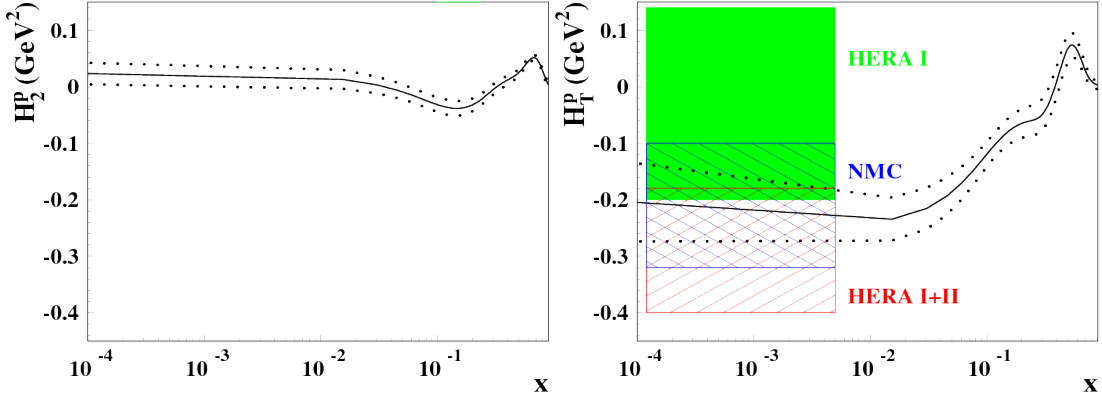


**Figure 3:** The coefficients of HT contribution to the proton DIS structure function  $F_2$  (left panel) and  $F_T$  (right panel) obtained in the present analysis (solid line: central value, dots:  $1/\sigma$  error band). The low- $x$  asymptotic of the HT terms preferred by various data sets (shaded area: HERA Run I, left-tilted hatches: NMC, shaded area: HERA Run I, right-tilted hatches: HERA Run I+II) is given for comparison.

$x \gtrsim 0.01$ . In the region of  $x \lesssim 0.01$  controlled by the HERA and NMC data sets the HT coefficients obtained in the ABM12 analysis are consistent with zero within uncertainties and therefore were set to zero. However, replacement of the HERA Run I data by the Run I+II ones leads to a change in this trend, cf. Fig. 3. As a result the HT coefficients in the structure function  $F_T$  obtained in the present analysis do not vanish down to  $x \sim 10^{-4}$ . At the same time the small- $x$  HT terms in the structure function  $F_2$  are still compatible with zero. This relation implies a pronounced manifestation of the HT contribution to the structure function  $F_L = F_2 - F_T$ , in line with the earlier observation [12].

The heavy-quark masses are also considered as free parameters of present fit and are determined simultaneously with the PDFs and  $\alpha_s$ . Throughout we employ the running-mass definition which provides an improved perturbative stability as compared to the on-shell-mass case [1, 13]. In this way we obtain the  $\overline{MS}$ -values of  $m_c(m_c) = 1.252 \pm 0.018$  GeV and  $m_b(m_b) = 3.83 \pm 0.12$  GeV driven by the data on  $c$ - and  $b$ -quark semi-inclusive DIS production, respectively, in combination with the inclusive DIS data. Here the heavy-quark contribution is described within the framework of fixed-flavor-number (FFN) factorization scheme assuming that the heavy quarks are produced in the final state. This approach provides a good description of existing DIS data. Furthermore, the value of  $m_c$  obtained is in very good agreement with other determinations [10]. This contrasts with the results obtained in the variable-flavor-number (VFN) approach, which requires on-shell masses of  $m_c \sim 1.3$  GeV to provide a satisfactory data description [3, 4, 5]. This value is far below other determinations. Therefore it should be rather considered as a tuning parameter somehow curing the VFN scheme effects at low  $Q^2$  scales [14]. The Tevatron and LHC data on the inclusive single-top and top-pair production cross section employed in the present analysis allow to determine the  $t$ -quark mass as well. A theoretical description of these data is based on the Hathor framework [15, 16] including the NNLO corrections to the  $t\bar{t}$  and the  $t$ -channel single-top production [17, 18] and the approximate NNLO corrections to the  $s$ -channel single-top production [19]. The value of  $m_t(m_t) = 160.9 \pm 1.1$  GeV is obtained from the fit to all existing data including the

most recent LHC results for the collision energy of 13 TeV. The value of  $\alpha_s(M_Z) = 0.1147 \pm 0.0008$  found with the  $t$ -quark data added is somewhat larger than the one preferred by the DIS data, however, the difference is well within the uncertainties.

In conclusion, we have present an updated version of the ABM12 PDFs with improved quark separation and the strange sea determination, tuned to the recent data on the DY process, DIS, neutrino-induced charm production, and the  $t$ -quark production collected at the LHC, Tevatron, HERA, and CERN-SPS. The values of  $\alpha_s$  and the heavy quark masses are determined from the fit simultaneously with the PDFs and allow to validate the theoretical framework used.

## References

- [1] S. Alekhin, J. Blümlein and S. Moch, Phys. Rev. D **89** (2014) no.5, 054028 [arXiv:1310.3059 [hep-ph]].
- [2] S. Alekhin, J. Blümlein, S. Moch and R. Placakyte, arXiv:1508.07923 [hep-ph].
- [3] S. Dulat *et al.*, Phys. Rev. D **93** (2016) no.3, 033006 [arXiv:1506.07443 [hep-ph]].
- [4] L. A. Harland-Lang, A. D. Martin, P. Motylinski and R. S. Thorne, Eur. Phys. J. C **75** (2015) no.5, 204 [arXiv:1412.3989 [hep-ph]].
- [5] R. D. Ball *et al.* [NNPDF Collaboration], JHEP **1504** (2015) 040 [arXiv:1410.8849 [hep-ph]].
- [6] A. Accardi, L. T. Brady, W. Melnitchouk, J. F. Owens and N. Sato, Phys. Rev. D **93** (2016) no.11, 114017 [arXiv:1602.03154 [hep-ph]].
- [7] P. Jimenez-Delgado and E. Reya, Phys. Rev. D **89** (2014) no.7, 074049 [arXiv:1403.1852 [hep-ph]].
- [8] S. Camarda *et al.* [HERAFitter developers' Team Collaboration], Eur. Phys. J. C **75** (2015) no.9, 458 [arXiv:1503.05221 [hep-ph]].
- [9] S. Alekhin, J. Blümlein, L. Caminada, K. Lipka, K. Lohwasser, S. Moch, R. Petti and R. Placakyte, Phys. Rev. D **91** (2015) no.9, 094002 [arXiv:1404.6469 [hep-ph]].
- [10] K. A. Olive *et al.* [Particle Data Group Collaboration], Chin. Phys. C **38** (2014) 090001.
- [11] S. Alekhin, J. Blümlein and S. Moch, Phys. Rev. D **86** (2012) 054009 [arXiv:1202.2281 [hep-ph]].
- [12] I. Abt, A. M. Cooper-Sarkar, B. Foster, V. Myronenko, K. Wichmann and M. Wing, Phys. Rev. D **94** (2016) no.3, 034032 [arXiv:1604.02299 [hep-ph]].
- [13] S. Alekhin and S. Moch, Phys. Lett. B **699** (2011) 345 [arXiv:1011.5790 [hep-ph]].
- [14] A. Accardi *et al.*, Eur. Phys. J. C **76** (2016) no.8, 471 [arXiv:1603.08906 [hep-ph]].
- [15] M. Aliev, H. Lacker, U. Langenfeld, S. Moch, P. Uwer and M. Wiedermann, Comput. Phys. Commun. **182** (2011) 1034 [arXiv:1007.1327 [hep-ph]].
- [16] P. Kant, O. M. Kind, T. Kintscher, T. Lohse, T. Martini, S. Mölbitz, P. Rieck and P. Uwer, Comput. Phys. Commun. **191** (2015) 74 [arXiv:1406.4403 [hep-ph]].
- [17] M. Czakon, P. Fiedler and A. Mitov, Phys. Rev. Lett. **110** (2013) 252004 [arXiv:1303.6254 [hep-ph]].
- [18] M. Brucherseifer, F. Caola and K. Melnikov, Phys. Lett. B **736** (2014) 58 [arXiv:1404.7116 [hep-ph]].
- [19] S. Alekhin, S. Moch and S. Thier, arXiv:1608.05212 [hep-ph].

Experiment	ATLAS		CMS		D0		LHCb			
	7	13	7	8	1.96	7	7	8	8	
$\sqrt{s}$ (TeV)										
Final states	$W^+ \rightarrow l^+ \nu$	$W^+ \rightarrow l^+ \nu$	$W^+ \rightarrow \mu^+ \nu$	$W^+ \rightarrow \mu^+ \nu$	$W^+ \rightarrow \mu^+ \nu$	$W^+ \rightarrow \mu^+ \nu$	$W^+ \rightarrow \mu^+ \nu$	$Z \rightarrow e^+ e^-$	$W^+ \rightarrow \mu^+ \nu$	
	$W^- \rightarrow l^- \nu$	$W^- \rightarrow l^- \nu$	$W^- \rightarrow \mu^- \nu$	$W^- \rightarrow \mu^- \nu$	$W^- \rightarrow \mu^- \nu$	$W^- \rightarrow \mu^- \nu$	$W^- \rightarrow \mu^- \nu$		$W^- \rightarrow \mu^- \nu$	
	$Z \rightarrow l^+ l^-$	$Z \rightarrow l^+ l^-$				$Z \rightarrow \mu^+ \mu^-$	$Z \rightarrow \mu^+ \mu^-$		$Z \rightarrow \mu^+ \mu^-$	
Cut on the lepton $P_T$	$P_T^l > 20$ GeV	$P_T^l > 25$ GeV	$P_T^l > 25$ GeV	$P_T^l > 25$ GeV	$P_T^l > 25$ GeV	$P_T^l > 25$ GeV	$P_T^l > 20$ GeV	$P_T^e > 20$ GeV	$P_T^l > 20$ GeV	
<i>NDP</i>	30	6	11	22	10	13	31	17	32	
present analysis	31.0	9.2	22.4	16.5	17.6	19.0	45.1	21.7	40.0	
CJ15	-	-	-	-	20	29	-	-	-	
CT14	42	-	- <sup>a</sup>	-	-	34.7	-	-	-	
JR14	-	-	-	-	-	-	-	-	-	
HERAFitter	-	-	-	-	13	19	-	-	-	
MMHT14	39	-	-	-	21	-	-	-	-	
NNPDF3.0	35.4	-	18.9	-	-	-	-	-	-	

**Table 1:** The data on  $W^-$  and  $Z$ -production in  $pp$  and  $\bar{p}p$  collisions and the  $\chi^2$  values obtained for these data sets in the present analysis. The values obtained in the CJ15 [6], CT14 [3], JR14 [7], HERAFitter [8], MMHT14 [4], and NNPDF3.0 [5] analyses are given for comparison, if available.

<sup>a</sup>Statistically less significant data with the cut of  $P_T^l > 35$  GeV are used.